Contribution from the Departament de Quimica Inorgânica, Facultat de Ciencies Quimiques, Universitat de València, 46100 Burjassot (València), Spain, Laboratoire de Chimie Inorganique, ERA No. 672, Université de Paris-Sud, 91405 Orsay, France, and Laboratoire de Chimie des Métaux de Transition, Université de Pierre et Marie Curie, 75230 Paris, France

Oxamidato Complexes. 1. A Study of the Formation of Complexes between Copper(II) and H_2pmox (H_2pmox = *N*,*N*'-Bis(2-pyridylmethyl)oxamide). Synthesis, Crystal Structure, and Magnetic Properties of the Alternating-Chain Compound $[Cu_2(pmox)(H_2pmox)(H_2O)_2](NO_3)_2 \cdot 8H_2O$

Francesc Lloret,[1a] Miguel Julve,*[,1a] Juan Faus,[1a] Yves Journaux,*[,1b] Michèle Philoche-Levisalles,[1c] and Yves Jeannin[1c]

Received December 18, 1988

The complexing of copper(II) by the ligand *N*,*N*'-bis(2-pyridylmethyl)oxamide (H_2pmox, H_2L) has been investigated by potentiometry in aqueous solutions at 25 °C and 0.1 mol dm^{-3} $NaNO_3$. The equilibrium constant for the formation of $[Cu_2(pmox)]^{2+}$ was found to be $\log \beta = 26.1$ (1) whereas the proton association constants corresponding to the equilibria $2H^+ + L^{2-} \rightleftharpoons H_2L$, $H^+ + H_2L \rightleftharpoons H_3L^+$, and $2H^+ + H_2L \rightleftharpoons H_4L^{2+}$ were 23.7 (1), 4.37 (1) and 7.95 (1) for $\log \beta$ of the three equilibria, respectively. The title compound has been synthesized, and its crystal structure has been determined at 298 K. The compound crystallizes in the triclinic system, space group $P\bar{1}$, with $a = 9.767$ (2) Å, $b = 10.668$ (2) Å, $c = 10.767$ (2) Å, $\alpha = 100.00$ (1)°, $\beta = 105.49$ (1)°, $\gamma = 106.95$ (1)°, $V = 995$ (1) Å^3, and $Z = 1$. The structure consists of cationic zigzag chains of copper atoms bridged by the neutral ligand H_2pmox and its deprotonated form $pmox^{2-}$. The electroneutrality is achieved by noncoordinated nitrate counterions. The coordination environment around the copper(II) ions, which are related by inversion centers lying on the L^{2-} and H_2L ligands, can be described as a distorted octahedron. The equatorial plane is defined by the N(1) and O(1) atoms of the deprotonated amide and N(2) and N(3) nitrogen atoms of pyridine groups belonging to L^{2-} and H_2L, respectively. The axial positions are occupied by an oxygen atom (O(3)) of a water molecule and a nitrogen atom (N(4)) of the amide group of H_2L ligand. The decrease of the magnetic susceptibility per two copper(II) ions versus the temperature is indicative of a large antiferromagnetic interaction. Although the crystal structure suggests an alternating linear chain, it has been possible to interpret the data with a simple Bleaney-Bowers equation. The relevant parameters are $g = 2.16$ and $J = -578$ cm^{-1} with the interaction Hamiltonian defined as $\hat{H} = -J\hat{S}_1 \cdot \hat{S}_2$. EPR data are consistent with this interpretation, showing that the alternating-chain description is not valid to describe its magnetic behavior. The singlet-triplet gap is compared to the reported ones for related systems and discussed in the framework of a simple orbital model.

Introduction

Although the first experimental studies on one-dimensional magnets were reported nearly 20 years ago,[2,3] major developments have occurred in both theoretical and experimental areas of this research field during the last decade. A lot of work has been carried out on the magnetic properties of linear-chain compounds,[4-6] and particular attention has been paid to alternating chains due mainly to their close connection with the spin-Peierls transition. Properties of many of the known alternating-chain systems are summarized in a recent review on significant advances in one-dimensional coordination compounds.[7] One of the strategies to synthesize homometallic alternating chains is that of reacting metal ions with two different potentially bridging ligands to yield structures of the type

$$-X'-M-X-M-X'-M-$$

However, a rarer situation is the one in which such a situation is achieved by using the same ligand in different degree of protonation, as is reported in this paper.

In the framework of a study of a series of copper(II) complexes bridged by extended ligands such as oxalato,[8] oxamato,[9] oxamidato,[9,10] and bipyrimidine,[11] we have investigated the formation of complexes between copper(II) and *N*,*N*'-bis(2-pyridylmethyl)oxamide (H_2pmox; hereafter abbreviated as H_2L) both in solution and in the solid state. We wish to report here on the complexing ability of this ligand toward hydrogen (basicity) and copper(II) in aqueous solution. The X-ray crystal structure of $[Cu_2L(H_2L)(H_2O)_2](NO_3)_2 \cdot 8H_2O$ together with a description of its magnetic properties are also presented.

Experimental Section

Materials. All chemicals were of reagent grade and were used without further purification. Carbonate-free NaOH (0.1 mol dm^{-3}) and HNO_3 (0.1 mol dm^{-3}) were used in the potentiometric titrations. All potentiometric measurements were carried out in 0.1 mol dm^{-3} $NaNO_3$ as ionic medium. H_2L was synthesized by following the procedure described in ref 12.

Preparation of the Crystals. Blue-green prismatic crystals of the title compound suitable for X-ray analysis have been obtained from aqueous solutions of 540 mg (2 mmol) of H_2L and 482 mg (2 mmol) of copper(II) nitrate trihydrate (25 mL) at pH = 3.50 by slow evaporation at room temperature. They were isolated, washed with cold water, and air-dried. Anal. Calcd for $C_{14}H_{23}N_5O_{10}Cu$: C, 34.68; H, 4.78; N, 14.44. Found: C, 34.69; H, 4.01; N, 14.41.

Physical Techniques. IR spectra were recorded on a Perkin-Elmer 1750 FTIR spectrophotometer as KBr pellets. Reflectance spectra were run on a Perkin-Elmer Lambda 9 spectrophotometer as Nujol mulls on filter paper.

Magnetic measurements were carried out in the 100-290 K temperature range by means of a Faraday-type magnetometer equipped with a helium-flow cryostat. The polycrystalline powder sample weighed about 14 mg. The independence of the susceptibility against the magnetic field was checked at room temperature. Mercury tetrakis(thiocyanato)cobaltate(II) was used as a susceptibility standard. Corrections for the diamagnetism of the title compound were estimated from Pascal constants as -484×10^{-6} cm^3 mol^{-1}.

(1) (a) Universitat de València. (b) Université de Paris-Sud. (c) Université de Pierre et Marie Curie.
(2) Dingle, R.; Lines, M. E.; Holt, S. L. *Phys. Rev.* **1969**, *187*, 643.
(3) Smith, T.; Friedberg, S. A. *Phys. Rev.* **1968**, *176*, 660.
(4) Hatfield, W. E. *J. Appl. Phys.* **1981**, *52*, 1985.
(5) Bonner, J. C. In *Magneto-Structural Correlations in Exchange Coupled Systems*; Willett, R. D., Gatteschi, D., Kahn, O., Eds.; NATO ASI Series 140; Reidel: Dordrecht; The Netherlands, 1985; p 157.
(6) Willett, R. D.; Gaura, R. M.; Landee, C. P. In *Extended Linear Chain Compounds*; Miller, J. S., Ed.; Plenum Press: New York, 1983; Vol. 3, p 143.
(7) Landee, P. In *Organic and Inorganic Low-Dimensional Crystalline Materials*; Delhaes, P., Drillon, M., Eds.; Plenum Press: New York and London, 1987; p 75.
(8) (a) Julve, M.; Verdaguer, M.; Kahn, O.; Gleizes, A.; Philoche-Levisalles, M. *Inorg. Chem.* **1983**, *22*, 368. (b) *Ibid.* **1984**, *23*, 3808.
(9) Verdaguer, M.; Kahn, O.; Julve, M.; Gleizes, A. *Nouv. J. Chim.* **1985**, *9*, 325.
(10) Journaux, Y.; Sletten, J.; Kahn, O. *Inorg. Chem.* **1985**, *24*, 4063.
(11) Julve, M.; De Munno, G.; Bruno, G.; Verdaguer, M. *Inorg. Chem.* **1988**, *27*, 3160.
(12) Ojima, H.; Yamada, K. *Bull. Chem. Soc. Jpn.* **1970**, *43*, 3018.

0020-1669/89/1328-3702$01.50/0

Table I. Crystallographic Data for $[Cu_2(L)(H_2L)(H_2O)_2](NO_3)_2 \cdot 8H_2O$

chem formula	$C_{28}H_{46}N_{10}Cu_2O_{20}$
a, Å	9.767 (2)
b, Å	10.668 (2)
c, Å	10.767 (2)
α, deg	100.00 (1)
β, deg	105.49 (1)
γ, deg	106.95 (1)
V, Å^3	995 (1)
Z	1
fw	969.8
space group	$P\bar{1}$
T, °C	25
λ, Å	0.71073
ρ_{calcd}, g cm^{-3}	1.62
μ, cm^{-1}	11.6
transm coeff	1.00–0.97
$R = \sum\|\Delta F\|/\sum\|F_o\|$	0.0329
$R_w{}^a = [\sum w(\Delta F)^2/\sum wF_o^2]^{1/2}$	0.0355

[a] Unit weights.

Table II. Atomic Coordinates and Thermal Parameters[a,b] for Non-Hydrogen Atoms of $[Cu_2L(H_2L)_2(H_2O)_2](NO_3)_2 \cdot 8H_2O$

atom	x/a	y/b	z/c	10^4U_{eq}, Å^2
Cu(1)	−0.28165 (5)	−0.17687 (5)	−0.11288 (5)	238
O(1)	−0.1197 (3)	−0.0545 (3)	−0.1699 (2)	252
O(2)	−0.6605 (3)	−0.0952 (3)	−0.1407 (3)	349
O(3)	−0.1998 (3)	−0.3565 (3)	−0.1824 (3)	375
O(4)	−0.1296 (3)	−0.7638 (3)	−0.0178 (3)	423
O(5)	0.0453 (3)	−0.6278 (3)	−0.0688 (3)	466
O(6)	−0.1671 (4)	−0.7517 (4)	−0.2209 (3)	584
O(7)	−0.0438 (4)	−0.6958 (3)	0.2964 (3)	505
O(8)	−0.0152 (4)	−0.1995 (4)	0.4840 (3)	601
O(9)	−0.1823 (4)	−0.0381 (4)	−0.4458 (3)	535
O(10)	−0.1111 (4)	−0.4557 (4)	0.2894 (3)	593
N(1)	−0.1294 (3)	−0.0913 (3)	0.0618 (3)	245
N(2)	−0.4028 (3)	−0.2608 (3)	−0.0009 (3)	264
N(3)	−0.4535 (3)	−0.2417 (3)	−0.2883 (3)	255
N(4)	−0.4210 (3)	0.0184 (3)	−0.1307 (3)	294
N(5)	−0.0858 (4)	−0.7149 (3)	−0.1029 (3)	361
C(1)	0.00004 (4)	−0.0090 (4)	−0.0681 (3)	226
C(2)	−0.1633 (4)	−0.1254 (4)	0.1778 (4)	272
C(3)	−0.3251 (4)	−0.2208 (4)	0.1314 (3)	239
C(4)	−0.3938 (4)	−0.2636 (4)	0.2224 (4)	315
C(5)	−0.5430 (5)	−0.3485 (5)	0.1761 (4)	358
C(6)	−0.6227 (4)	−0.3894 (4)	0.0397 (4)	332
C(7)	−0.5489 (4)	−0.3445 (4)	−0.0449 (4)	306
C(8)	−0.5120 (4)	−0.3762 (4)	−0.3491 (4)	336
C(9)	−0.6365 (5)	−0.4349 (5)	−0.4658 (4)	390
C(10)	−0.7005 (5)	−0.3512 (5)	−0.5232 (4)	396
C(11)	−0.6420 (4)	−0.2142 (5)	−0.4628 (4)	360
C(12)	−0.5200 (4)	−0.1615 (4)	−0.3435 (3)	264
C(13)	−0.4595 (4)	−0.0119 (4)	−0.2752 (4)	321
C(14)	−0.5291 (4)	−0.0236 (4)	−0.0769 (3)	249

[a] Estimated standard deviations in the last significant digits are given in parentheses. [b] $U_{eq} = {}^1/_3\sum_i\sum_j U_{ij}a^*_i a^*_j \mathbf{a}_i \mathbf{a}_j$.

The X-band EPR spectra were recorded in the same temperature range by means of a Bruker ER 200 D spectrometer equipped with an Oxford Instruments continuous-flow cryostat. The magnetic field was determined with a Hall probe and the klystron frequency with a Hewlett-Packard frequency meter.

The potentiometric titrations were carried out by using a reaction vessel (capacity 70 cm^3) water thermostated at 25.0 ± 0.1 °C. The titrant was delivered by a Crison 738 buret. The emf measurements were performed by using a Radiometer PHM 84 pH-mV meter, and a 9811 Ingold combined glass electrode. The titration system was controlled by an Apple IIe microcomputer. A Basic program[13] was used to monitor for each titration point, the emf values, and the volume of titrant added. When the observed emf value was constant, within user-defined limits, the next volume of titrant was added automatically and the cycle repeated until the predefined total volume of titrant had been added. The computer program SUPERQUAD[14] was used to process data and calculate both basicity and stability constants. Accurate concentrations of the basic titrant as well as the $E^{\circ\prime}$ values were determined by applying Gran's method with a nitric acid solution previously standardized with tris(hydroximethyl)aminomethane[15] before each titration series. Metal to ligand ratios in the range 0.5–2 were used in the study of complex formation (c_M = (5–1) × 10^{-3} mol dm^{-3}).

Table III. Main Bond Distances (Å) and Bond Angles (deg)[a,b] for $[Cu_2L(H_2L)(H_2O)_2](NO_3)_2 \cdot 8H_2O$

Bond Distances			
Cu(1)–N(3)	2.010 (3)	Cu(1)–N(1)	1.924 (3)
Cu(1)–N(2)	2.043 (3)	Cu(1)–O(1)	2.043 (2)
Cu(1)–O(3)	2.364 (3)	Cu(1)–N(4)	2.807 (3)
N(3)–C(12)	1.342 (5)	N(3)–C(8)	1.346 (5)
N(4)–C(13)	1.452 (5)	N(4)–C(14)	1.339 (5)
N(1)–C(1)	1.286 (4)	N(1)–C(2)	1.452 (4)
N(2)–C(3)	1.346 (4)	N(2)–C(7)	1.345 (4)
C(12)–C(11)	1.388 (5)	C(12)–C(13)	1.499 (5)
C(11)–C(10)	1.367 (6)	C(10)–C(9)	1.372 (6)
C(9)–C(8)	1.384 (5)	C(14)–C(14)^{ii}	1.536 (7)
C(14)–O(2)	1.216 (4)	C(1)–C(1)^{i}	1.513 (7)
C(1)–O(1)	1.276 (4)	C(2)–C(3)	1.499 (5)
C(3)–C(4)	1.394 (5)	C(7)–C(6)	1.371 (5)
C(6)–C(5)	1.387 (6)	C(5)–C(4)	1.371 (5)
N(5)–O(4)	1.241 (4)	N(5)–O(5)	1.255 (4)
N(5)–O(6)	1.227 (4)		
Bond Angles			
N(1)–Cu(1)–N(3)	170.6 (1)	N(2)–Cu(1)–N(3)	97.7 (1)
N(3)–Cu(1)–N(4)	71.0 (1)	N(2)–Cu(1)–N(1)	81.1 (1)
O(1)–Cu(1)–N(3)	97.9 (1)	O(1)–Cu(1)–N(1)	82.4 (1)
O(1)–Cu(1)–N(2)	162.8 (1)	O(3)–Cu(1)–N(3)	90.4 (1)
O(3)–Cu(1)–N(1)	99.0 (1)	O(3)–Cu(1)–N(2)	99.5 (1)
O(3)–Cu(1)–O(1)	87.5 (1)	N(1)–Cu(1)–N(4)	99.7 (1)
N(2)–Cu(1)–N(4)	92.1 (1)	O(1)–Cu(1)–N(4)	86.3 (1)
O(3)–Cu(1)–N(4)	159.3 (1)	C(8)–N(3)–C(12)	118.2 (3)
C(14)–N(4)–C(13)	120.2 (3)	C(1)–N(1)–Cu(1)	117.1 (2)
C(2)–N(1)–C(1)	119.2 (2)	C(2)–N(1)–C(1)	123.6 (3)
C(3)–N(2)–Cu(1)	114.1 (2)	C(7)–N(2)–Cu(1)	127.2 (3)
C(2)–N(1)–Cu(1)	119.2 (2)	C(7)–N(2)–C(3)	118.7 (3)
C(11)–C(12)–N(3)	121.3 (4)	C(13)–C(12)–N(3)	119.0 (3)
C(13)–C(12)–C(11)	119.7 (4)	C(10)–C(11)–C(12)	119.9 (4)
C(9)–C(10)–C(11)	119.5 (4)	C(8)–C(9)–C(10)	118.2 (4)
C(9)–C(8)–N(3)	123.0 (4)	C(12)–C(13)–N(4)	113.2 (3)
C(14)^{ii}–C(14)–N(4)	113.5 (4)	O(2)–C(14)–N(4)	124.6 (3)
O(2)–C(14)–C(14)^{ii}	121.8 (4)	C(1)^{i}–C(1)–N(1)	111.8 (4)
O(1)–C(1)–N(1)	129.0 (3)	O(1)–C(1)–C(1)^{i}	119.2 (4)
C(3)–C(2)–N(1)	108.1 (3)	C(2)–C(3)–N(2)	117.5 (3)
C(4)–C(3)–N(2)	121.2 (3)	C(4)–C(3)–C(2)	121.2 (3)
C(6)–C(7)–N(2)	122.7 (4)	C(5)–C(6)–C(7)	118.8 (3)
C(4)–C(5)C(6)	119.1 (4)	C(5)–C(4)–C(3)	119.4 (4)
O(5)–N(5)–O(4)	119.7 (3)	O(6)–N(5)–O(4)	121.4 (3)
O(6)–N(5)–O(5)	118.9 (3)	C(8)–N(3)–Cu(1)	117.3 (3)
C(12)–N(3)–Cu(1)	124.4 (3)	C(1)–O(1)–Cu(1)	109.3 (2)

[a] Estimated standard deviations in the last significant digits are given in parentheses. [b] Roman numeral superscripts refer to the following equivalent positions relative to x, y, z: (i) $\bar{x}$, $\bar{y}$, $\bar{z}$; (ii) $-1-x$, $\bar{y}$, $\bar{z}$.

X-ray Data Collection and Structure Refinement. Diffraction data were collected on a CAD4 Enraf Nonius diffractometer, using graphite-monochromated Mo Kα radiation (λ = 0.71069 Å). Accurate unit-cell parameters were obtained from least-squares refinement of 25 reflections in the 14–16° θ range. They are listed in Table I along with other relevant crystallographic details. A full-length table of crystallographic data is given as supplementary material (Table SI). The intensities of two standard reflections measured every 2 h showed no significant variations. Intensity data were collected by the θ–2θ scan technique in the 2θ range 2–50°. Empirical absorption correction using the Ψ scan of two reflections was applied. Of the 3505 measured independent reflections, 2388 were unique with $F \geq 3\sigma(F)$ and were used for the structure refinement. The copper atom was located on a Patterson map, and all other atoms were found in subsequent Fourier maps. Least-squares refinements were carried out in four blocks (273 parameters) with anisotropic thermal parameters for all non-hydrogen atoms. Hydrogen atoms were located from ΔF map but not refined. An isotropic temperature factor was assigned to them. The function minimized was

(13) Mollar, M. Ph.D. Thesis, University of València, Spain, 1988.

(14) Gans, P.; Sabatini, A.; Vacca, A. *J. Chem. Soc., Dalton Trans.* **1985**, 1195.

(15) Subert, J. *Farm. Obz.* **1980**, *49*, 71.

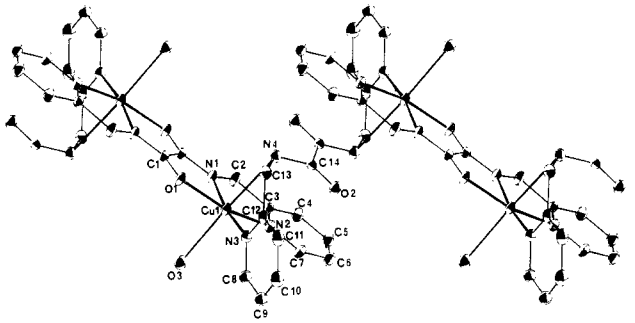

Figure 1. ORTEP view of the asymmetric unit and of three symmetry-related units of $[Cu_2L(H_2L)_2(H_2O)_2](NO_3)_2 \cdot 8H_2O$. Thermal ellipsoids are drawn at the 30% probability level, and hydrogen atoms are not shown for simplicity.

$\sum w(|F_o| - |F_c|)^2$. Each reflection was assigned a unity weight, and a secondary extinction coefficient (32×10^{-4}) was introduced in the final stage of the refinement. The scattering factors for all atoms and the anomalous dispersion correction term for Cu were taken from ref 16. The computer program CRYSTALS[16] was used in the crystallographic calculations. The final values of the discrepancy indices, R and R_w were 0.0329 and 0.0355, respectively. The final difference-Fourier map shows residual maxima and minima of 0.35 and −0.31 e Å^{-3}. Refined positional parameters for non-hydrogen atoms and main bond distances and angles are given in Tables II and III, respectively. Anisotropic thermal parameters, positional parameters for hydrogen atoms, least-squares planes, and observed and calculated structure factors (Tables SII–V) are available as supplementary material.

Results and Discussion

Description of the Structure. The crystal structure of $[Cu_2L(H_2L)(H_2O)_2](NO_3)_2 \cdot 8H_2O$ is made up of cationic zigzag chains of copper atoms bridged by both H_2L and L^{2-} ligands, noncoordinated nitrate ions, and coordinated and noncoordinated water molecules. A perspective view of the asymmetric unit along with the atom-labeling scheme and of three symmetry-related units is shown in Figure 1. Inversion centers stand at the middle of the C(1)–C(1)^{i} and C(14)–C(14)^{ii} bonds of the deprotonated and neutral amide, respectively.

The copper(II) ion is in a distorted octahedral surrounding. The equatorial plane is defined by the oxygen (O(1)) and nitrogen (N(1)) atoms of the deprotonated amide and two pyridyl nitrogen atoms of the deprotonated (N(2)) and neutral (N(3)) amide. The mean displacement of the four atoms from this plane is 0.028 (5) Å. The copper atom lies 0.131 (1) Å out of this mean basal plane. The Cu–N(1) bond distance is significantly shorter (1.924 (3) Å) than the other three equatorial distances (2.010 (3), 2.043 (3), and 2.043 (2) Å for Cu–N(3), Cu–N(2) and Cu–O(1), respectively) but close to those found in three analogous copper complexes with oxamides.[9,17] The axial coordination sites are occupied by an oxygen atom (O(3)) of a water molecule and a nitrogen atom (N(4)) of the neutral H_2L ligand at greater distances: Cu–O(3) = 2.364 (3) Å and Cu–N(4) = 2.807 (3) Å. The N(4)–Cu–O(3) angle is 159.3 (1)° whereas the N(3)–Cu–N(1) and N(2)–Cu–O(1) ones are 170.6 (1) and 162.8 (1)°, respectively.

The pyridyl rings of both H_2L and L^{2-} show no significant deviation from planarity. The deprotonated amide ligand is almost planar (largest deviation from the mean plane defined by C(1), O(1), N(1), C(2), C(3), C(4), C(5), C(6), C(7), and N(2) is 0.083 (7) Å for N(2)) whereas for the neutral amide ligand, the oxamide group (N(4), C(14), O(2)) and the pyridyl ring make a dihedral angle of 96.8 (4)°. The interplanar angle between the N(3), C(8), C(9), C(10), C(11), and C(12) and N(2), C(3), C(4), C(5), C(6), and C(7) pyridyl rings is 107.2 (5)°. The torsional angle for the C(13)–N(4) linkage is 62.7 (4)° where the corresponding one for the C(2)–N(1) bond is only 3.7 (4)°.

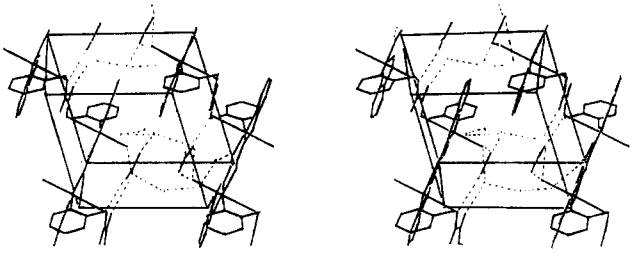

Figure 2. Stereoscopic view of the cell of $[Cu_2L(H_2L)(H_2O)_2](NO_3)_2 \cdot 8H_2O$ down the c axis (b axis is horizontal). Hydrogen-bonding interactions are indicated by dotted lines.

Table IV. Hydrogen-Bonding Interactions[a] in $[Cu_2L(H_2L)(H_2O)_2](NO_3)_2 \cdot 8H_2O$

O(n)–H(n)···O(m)[a]	O(n)–O(m), Å	H(n)–O(m), Å
O(8)–H(19)···O(7)^{i}	2.781	1.86
O(3)–H(14)···O(5)^{ii}	2.783	1.93
O(7)–H(16)···O(10)	2.832	2.03
O(9)–H(21)···O(8)^{v}	2.836	2.09
O(10)–H(22)···O(5)^{ii}	2.840	1.99
O(8)–H(18)···O(10)	2.865	1.87
N(4)–H(13)···O(4)^{iii}	2.880	1.93
O(7)–H(17)···O(2)^{iv}	2.913	2.25
O(3)–H(15)···O(7)^{ii}	2.916	1.97
O(9)–H(20)···O(1)	2.916	2.14
O(9)···(08)^{vi}	2.872	

[a] Roman numeral superscripts refer to the following equivalent positions relative to x, y, z: (i) $-x, -y, -1, -z + 1$; (ii) $-x, -y - 1, -z$; (iii) $x, y + 1, z$; (iv) $-x - 1, -y - 1, -z$; (v) $x, y, z - 1$; (vi) $-x, -y, -z$.

The bis-tridentate character of the L^{2-} ligand produces two five-membered chelate metal cycles on each copper atom. The short bond angles around the metal ion in these five-membered rings (82.4 (1)° and 81.1 (1)° for O(1)–Cu–N(1) and N(1)–Cu–N(2), respectively) causes sensitive deviations from the ideal 90° value in the O(1)–Cu–N(3) (97.9 (1)°) and N(3)–Cu–N(2) (97.7 (1)°) angles. The intrachain copper–copper distances for the metal ions separated by the L^{2-} and H_2L ligands are 5.290 (1) and 7.077 (1) Å, respectively whereas the shortest interchain copper–copper separation is 8.114 (1) Å. The shortest copper–copper distance is the longest so far reported for copper complexes bridged by oxamidato ligands.[9,17-19]

A stereoview of the packing of the chains parallel to the a axis illustrating the network of hydrogen-bonding interactions that involve water molecules, nitrate ions, and cationic one-dimensional chains is depicted in Figure 2. A listing of hydrogen bonds is given in Table IV.

Infrared and Electronic Spectra. Bands of ionic nitrate[20] are located at 2430 (w), 1390 (s), and 830 (w) cm^{-1}. A band centered at 3420 (s, br) cm^{-1} reveals the presence of water. The IR spectrum in the N–H stretching region consists of a single absorption of medium intensity at 3290 cm^{-1}, which indicates the presence of N–H amide groups. This band had been observed for free H_2L ligand as a single intense band at the same wavenumber.[21] The amide I band is observed at 1650 cm^{-1} as a single peak, a value which is close to the observed ones for (μ-oxamidato)copper(II) complexes[22] and free H_2L. The occurrence of ν_s(CO) at 1530 (m) and 1340 (m) cm^{-1} supports the presence of H_2L and bridging oxamidato, respectively. All these spectral features agree with the structure described above.

The reflectance spectrum consists of a charge-transfer band centered at 24 700 cm^{-1} and a broad d–d band at 15 100 cm^{-1} with a shoulder at 10 600 cm^{-1}. These two last features are tentatively

(16) Carruthers, J. R.; Watkin, D. W. J. "CRYSTALS, an advanced crystallographic computer program"; University of Oxford: Chemical Crystallographic Laboratory, Oxford, England, 1985.
(17) Sletten, J. *Acta Chem. Scand., Ser A* **1982**, *36*, 345.
(18) Bencini, A.; Di Vaira, M.; Fabretti, A. C.; Gateschi, D.; Zanchini, C. *Inorg. Chem.* **1984**, *23*, 1620.
(19) Bencini, A.; Benelli, C.; Fabretti, A. C.; Franchini, G.; Gatteschi, D. *Inorg. Chem.* **1986**, *25*, 1063.
(20) Rosenthal, M. R. *J. Chem. Educ.* **1973**, *50*, 331.
(21) Ojima, H.; Nonoyama, K. *Z. Anorg. Allg. Chem.* **1977**, *429*, 282.
(22) (a) Ojima, H.; Nonoyama, K. *Z. Anorg. Allg. Chem.* **1972**, *389*, 75. (b) *Ibid.* **1973**, *401*, 195.

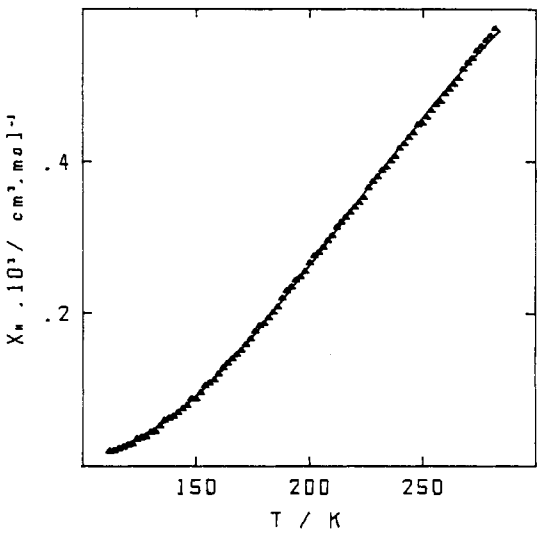

Figure 3. Temperature dependence of the magnetic susceptibility per two copper(II) ions of $[Cu_2L(H_2L)(H_2O)_2](NO_3)_2 \cdot 8H_2O$. Experimental points are represented by triangles whereas the solid line is the theoretical line obtained by least-squares fitting of all experimental points.

assigned as $d_{xy,xz,yz} \rightarrow d_{x^2-y^2}$ and $d_{z^2} \rightarrow d_{x^2-y^2}$, respectively. This choice may be supported by the fact that our complex could be considered as having a square-pyramidal stereochemistry (the Cu(1)–N(4) distance is somewhat longer than the Cu(1)–O(3) one) with a T value[23] of 0.848.

Magnetic Properties and EPR Data. The temperature dependence of the magnetic susceptibility per two copper atoms of $[Cu_2L(H_2L)(H_2O)_2](NO_3)_2 \cdot 8H_2O$ is shown in Figure 3. The decrease of χ with T in the 290–100 K temperature range is indicative of a very strong antiferromagnetic interaction between copper atoms. Considering the structure, two exchange pathways are possible: one through the deprotonated L^{2-} ligand and the other one through its neutral H_2L form. The unpaired electron of each copper(II) ion is described by a magnetic orbital that points toward the nearest neighbors (O(1), N(1), N(2), and N(3) atoms) in the plane of the deprotonated ligand. That rules out a strong interaction through the H_2L ligand, which is perpendicular to the plane of the magnetic orbital. On the other hand, oxamidato ligands are known to be very effective in transmitting the exchange interaction between two copper(II) ions when the magnetic orbitals are in the plane of the oxamidato ligand,[10,24,25] leading to interactions as large as -580 cm^{-1}.[9] Therefore, although the crystal structure suggests an alternating linear chain, the compound must behave magnetically as a chain of weakly interacting binuclear units. Consequently, in a first approach, we interpret the data with a simple Bleaney–Bowers equation. The curve calculated under this assumption fits very well with the experimental points as shown in Figure 3. Least-squares fit of the experimental data with the interaction Hamiltonian $\hat{H} = -J\hat{S}_1 \cdot \hat{S}_2$ leads to $J = -578$ cm^{-1} and $g = 2.16$ with $R = 9.5 \times 10^{-5}$ R is the agreement factor defined as $R = \sum_i (\chi_{obsd})_i - (\chi_{theor})_i)^2 / \sum_i (\chi_{obsd})_i^2$. The obtained J value is close to the reported ones for other structurally characterized (μ-oxamidato)copper(II) complexes[9,18] and significantly greater than the reported one for an alternating copper(II) chain containing acetate and *N,N'*-bis(2-(aminomethyl)-2-methylpropyl)oxamidate as bridging ligands.[19] In a second approach, we took into account a possible interaction through the H_2L ligand, and the magnetic data were fitted with the alternating-chain model by using the empirical expression proposed by Hatfield.[26] In the frame of this interpretation, values of -579 cm^{-1}, 0.048, and 2.18

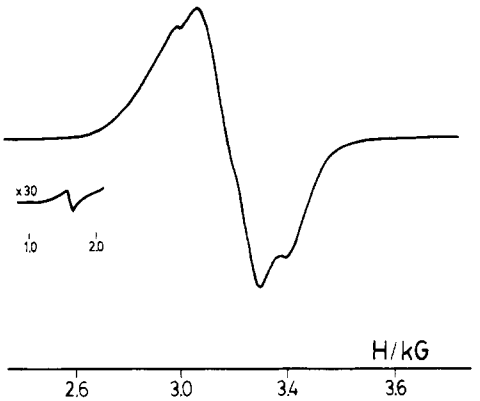

Figure 4. X-Band powder EPR spectra of $[Cu_2L(H_2L)(H_2O)_2](NO_3)_2 \cdot 8H_2O$ at room temperature.

were found for J, α (exchange alternating parameter), and g, respectively, with $R = 7.9 \times 10^{-5}$. By comparison with the previous model, the quality of the fit did not improve significantly and the J value, which corresponds to the interaction through the oxamidato bridge, remains practically unchanged. However, the value, which leads to $\alpha J = -28$ cm^{-1}, is unphysically large. As the magnetic data do not allow us to decide whether the description of the compound as an alternating chain is correct, we decided to take advantage of the complementarity between the EPR and the magnetic susceptibility measurements.[19,27] The polycrystalline powder EPR spectrum of $[Cu_2L(H_2L)(H_2O)_2](NO_3)_2 \cdot 8H_2O$ is shown in Figure 4. It presents a broad symmetric signal centered at 3200 G and a half-field transition at 1610 G. The central feature is the envelope of several transitions with two poorly resolved transitions at 2985 and 3393 G, and nonresolved transitions near 3130 and 3250 G. This spectrum is characteristic of a triplet spin state with the anisotropic zero-field splitting tensor. The presence of fine structure on it is indicative that αJ is smaller than the D value.[28] Indeed, one asymmetric feature with no fine structure is expected for an alternating chain.[19,28] It is now well established[29–31] that in binuclear copper(II) complexes the **g** and **D** tensors are not colinear, which makes difficult the interpretation of powder spectrum using the reported formulas for the transition fields along the principal axis.[32] Nevertheless, we could estimate a D value of 0.02 cm^{-1} by using the two resolved transitions at 2985 and 3393 G. This value is close to the expected dipolar contribution for two Cu(II) ions separated by 5.29 Å. However, a possible contribution of the anisotropic exchange interaction, which could be of the same order of magnitude for this kind of bridging ligand,[31] cannot be excluded without a single-crystal study.

The EPR as well as the magnetic susceptibility data are those of a binuclear compound. From the EPR spectra, it is possible to deduce that αJ is less than 0.02 cm^{-1}, showing that the alternating-chain description is not valid for the magnetic data. Therefore, the good fit obtained with the alternating-chain model is purely mathematical and has no physical meaning.

The J value of -578 cm^{-1} is a new confirmation of the remarkable efficiency of the oxamidato bridge to transmit the exchange interaction between two copper(II) ions relatively far from each other. This ability is the result of the weak electronegativity of nitrogen and the relatively short metal–nitrogen bond distances, which favor the spin delocalization on the bridge. The larger the spin delocalization on the bridge, the larger the overlap between

(23) Hataway, B. J.; Bew, M. J.; Billing, D. E.; Dudley, R. J.; Nicholls, P. *J. Chem. Soc. A* **1969**, 2312.
(24) Bencini, A.; Benelli, C.; Gatteschi, D.; Zanchini, C.; Fabretti, A. *Inorg. Chim. Acta* **1984**, *86*, 169.
(25) Berry, K. J.; Black, D. C. S.; Bos Vanderzalm, G. H.; Ian Moss, C.; Murray, K. S. *Inorg. Chim. Acta* **1984**, *86*, 169.
(26) Hatfield, W. E. *J. Appl. Phys.* **1981**, *52*, 1985.
(27) Journaux, Y.; Kahn, O.; Morgenstern-Badarau, I.; Galy, J.; Jaud, J.; Bencini, A.; Gatteschi, A. *J. Am. Chem. Soc.* **1985**, *107*, 6305.
(28) Blanc, J. P.; Dugay, M.; Robert, H.; Thibaud, C. *Phys. Status Solidi B* **1981**, *105*, 659.
(29) Banci, L.; Bencini, A.; Gatteschi, D. *J. Am. Chem. Soc.* **1983**, *105*, 761.
(30) Boillot, M. L.; Journaux, Y.; Bencini, A.; Gatteschi, D.; Kahn, O. *Inorg. Chem.* **1985**, *24*, 263.
(31) Bencini, A.; Fabretti, A.; Zanchini, C.; Zanini, P. *Inorg. Chem.* **1987**, *26*, 1445.
(32) Wasserman, E.; Snyder, L. C.; Yager, W. A. *J. Chem. Phys.* **1964**, *41*, 1763.

Table V. Equilibrium Data[a,b] for Basicity and Formation of Cu(II) Complexes with L^{2-} in Aqueous Solution (25 °C in 0.1 mol dm^{-3} $NaNO_3$)

reacn	log β
$2H^+ + L^{2-} \rightarrow H_2L$ (i)	23.7 (1)
$H^+ + H_2L \rightarrow H_3L^+$ (ii)	4.37 (1)
$2H^+ + H_2L \rightarrow H_4L^{2+}$ (iii)	7.95 (1)
$2Cu^{2+} + H_2L \rightarrow Cu_2L^{2+} + 2H^+$ (iv)	2.39 (1)
$2Cu^{2+} + L^{2-} \rightarrow Cu_2L^{2+}$ (v)	26.1 (1)[b]

[a] Values in parentheses are standard deviations in the last significant figure. [b] This value is obtained by combining eq i and iv.

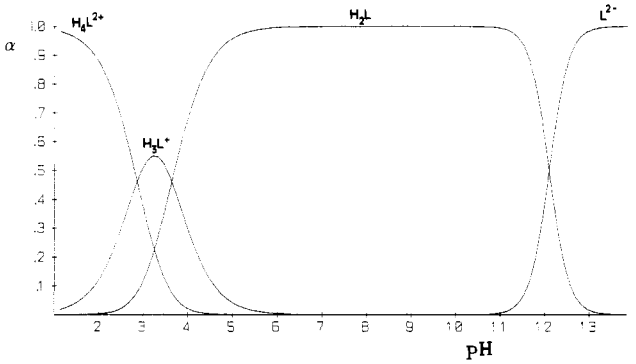

Figure 5. Distribution diagram for the system H^+/L^{2-}.

the magnetic orbitals is and the larger the antiferromagnetic coupling is.[9] On the other hand, the very small upper limit for the αJ value is not surprising owing to the Cu(II) magnetic orbitals orientation, which cannot lead to a strong overlap through the H_2L bridging ligand.

Solution Study. The protonation equilibrium constants of the ligand are given in Table V. These values show that such a ligand behaves as a relatively strong base in the two first protonation steps and that its basicity decreases as the degree of protonation increases. A marked difference in basicity is observed when comparing the protonation constant of 2-methylpyridine with the ones of the pyridyl groups of H_2L: 6.06 for the logarithm of the association constant of 2-methylpyridine[33] and 4.37 and 3.58 for the logarithms of the stepwise protonation constants of the pyridyl groups of H_2L. This is probably due to the existence of hydrogen bonds involving N–H amide groups and N-pyridinic atoms, which should be broken when protonation occurs. Obviously, such hydrogen-bonding interactions would decrease the basicity of the pyridyl rings of H_2L. On the other hand, the electrostatic repulsion between positively charged pyridinium groups explains the decrease of basicity when both pyridyl groups are protonated. The distribution diagram for the system H^+/L^{2-} is depicted in Figure 5. The predominant species at lower pH values are H_4L^{2+} and H_3L^+ whereas the concentration of H_2L becomes significant at pH > 3.40 being the only existing species in the range 5.70 ≤ pH ≤ 11. At pH > 11, the concentration of H_2L decreases to yield the species L^{2-} in which the amido groups are deprotonated. The determination of the deprotonation constants of the N–H amide groups by potentiometry in aqueous solution is not reliable because such a deprotonation occurs in very basic media. We have treated potentiometric data up to pH = 11.50, for which about 20% of L^{2-} is present, and we have obtained a value of 23.7 (1) for the logarithm of the overall protonation constant of the oxamidato groups. This value illustrates the high basicity of such groups.

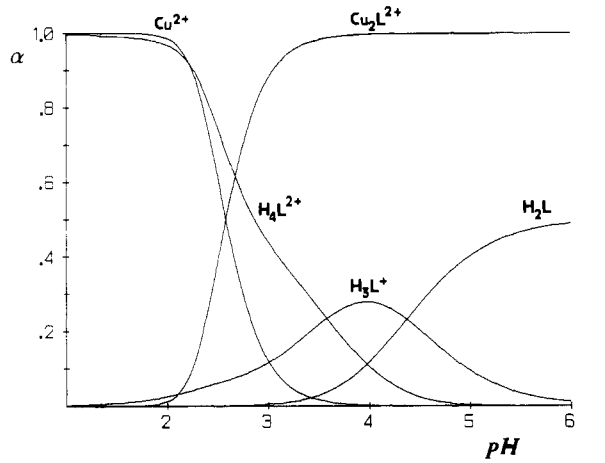

Figure 6. Distribution diagram for the system $Cu^{2+}/L^{2-}/H^+$ as a function of pH ($c_M = c_L = 5 \times 10^{-3}$ mol dm^{-3}). $[Cu_2L(H_2L)(H_2O)_2](NO_3)_2 \cdot 8H_2O$ precipitates at pH ≥ 3.50.

Work in progress on related ligands such as *N,N'*-bis(3-aminopropyl)oxamidate ($oxpn^{2-}$), *N,N'*-bis(2-carboxymethyl)oxamidate ($glyox^{4-}$), and *N,N'*-bis(3-carboxyethyl)oxamidate ($alanox^{4-}$) show values of the logarithm of the protonation constants of the amidate groups of 23.8, 24.2, and 24.1 respectively. All these values are very close, and the small differences they exhibit can be explained in terms of electrostatic interactions: the protonation of oxamidate groups leads to neutral species in the case of L^{2-} and $oxpn^{2-}$ and to dianions of $glyox^{4-}$ and $alanox^{4-}$ ligands.

The ligand L^{2-} forms a very stable binuclear complex with copper(II) $[Cu_2L]^{2+}$ (log β = 26.1 (1). The formation of such a species takes place in the 2–3.50 pH range (see Figure 6). The degree of formation of $[Cu_2L]^{2+}$ is 100% at pH = 3.50. Significant amounts of H_2L are present at this pH value and its bismonodentate coordination to the complex $[Cu_2L]^{2+}$ leads to the alternating chain $[Cu_2L(H_2L)(H_2O)_2]^{2+}$, which precipitates as a nitrate salt. The formation of other $Cu^{2+}:L^{2-}$ complexes could not be followed because this precipitation. However, it deserves to be pointed out that such a solid is readily soluble in more basic media, yielding the violet neutral mononuclear complex [CuL] that we have isolated as a monohydrate. The alternating-chain compound precipitates as chloride or perchlorate salts when $NaNO_3$ is substituted by NaCl or $NaClO_4$.

The formation constant of $[Cu_2L]^{2+}$ (log β = 26.1 (1)) is smaller than the corresponding one for the parent complex $[Cu_2(oxpn)]^{2+}$ (log β = 28.3)[34] but greater than the one of the complex $[Cu_2(glyox)]$ (log β = 22.0).[35] The sequence of the values of the stability constants of these binuclear complexes, glyox < pmox < oxpn, agrees with the known stability trend for copper(II) complexes, i.e. carboxylate < pyridine < amine.

Acknowledgment. This work was partially supported by the Comisión Interministerial de Ciencia y Tecnologia (Proyecto PB85-0190).

Supplementary Material Available: Listings of crystallographic data (Table SI), anisotropic thermal parameters (Table SII), hydrogen coordinates (Table SIII), and least-squares planes (Table SIV) (4 pages); a listing of calculated and observed structure factors (Table SV) (19 pages). Ordering information is given on any current masthead page. A listing of experimental magnetic data is available from the authors on request.

(33) Kahman, K.; Sigel, H.; Erlenmeyer, H. *Helv. Chim. Acta* **1964**, *47*, 1754.

(34) Ruiz, R.; Lloret, F.; Julve, M.; Faus, J. Unpublished results.

(35) Lloret, F.; Sletten, J.; Verdaguer, M.; Faus, J.; Julve, M. Manuscript in preparation.